







Error-Controllable Scheme for the LOD-FDTD Method

Tasuku Nakazawa , Di Wu , Seiya Kishimoto , *Member, IEEE*, Jun Shibayama , *Member, IEEE*, Junji Yamauchi , *Life Fellow, IEEE*, and Shinichiro Ohnuki , *Member, IEEE*

Abstract—The implicit locally one-dimensional finite-difference time-domain (LOD-FDTD) method is useful for designing plasmonic devices and waveguide structures. By using a large timestep size, the implicit LOD-FDTD method can reduce the computational time; however, this involves a trade-off with accuracy. To overcome this trade-off, we propose an error-controllable scheme for the LOD-FDTD method, wherein the fast inverse Laplace transform is employed to generate the electromagnetic field in arbitrary time domain from that in complex frequency domain. Compared to the conventional LOD-FDTD method, our scheme provides higher accuracy with more efficient calculations.

Index Terms—Error control, fast inverse laplace transform, finite-difference complex-frequency-domain method, finite-difference time-domain method, locally one-dimensional method, parallel computing, plasmonic device.

I. INTRODUCTION

TIME-domain analyses are essential for the design of electromagnetic devices. The numerical modeling of such devices with fine structures requires a small spatial mesh to ensure the reliability of finite difference methods. Thus, the traditional explicit finite-difference time-domain (FDTD) method [1], [2] is computationally expensive because of the constraint imposed by the Courant–Friedrichs–Lewy (CFL) condition, which is determined by cell size. To eliminate this restriction, implicit methods based on the locally one-dimensional (LOD) scheme [3] have been established. Because such approaches are unconditionally stable, there are no restrictions on timestep selection. They can be used to design plasmonic devices consisting of dispersive media with reduced computational time [4]. However, the numerical error of the LOD-FDTD method increases with the timestep size, where a significant spatial variation of the field exists, as seen in the singularity at the boundaries of different mediums.

Manuscript received March 8, 2022; revised May 4, 2022; accepted June 2, 2022. Date of publication June 10, 2022; date of current version June 23, 2022. This work was supported in part by the Japan Society for the Promotion of Science KAKENHI under Grant JP21K17753 and in part by the College of Science and Technology, Nihon University. (*Corresponding author: Shinichiro Ohnuki.*)

Tasuku Nakazawa, Di Wu, Seiya Kishimoto, and Shinichiro Ohnuki are with the College of Science and Technology, Nihon University, Chiyoda 101-8308, Japan (e-mail: csts20019@g.nihon-u.ac.jp; cste18001@g.nihon-u.ac.jp; kishimoto.seiya@nihon-u.ac.jp; ohnuki.shinichiro@nihon-u.ac.jp).

Jun Shibayama and Junji Yamauchi are with the Faculty of Science and Engineering, Hosei University, Koganei 184-8584, Japan (e-mail: shiba@hosei.ac.jp; j.yma@hosei.ac.jp).

Digital Object Identifier 10.1109/JMMCT.2022.3181568

In this study, we propose a novel approach for controlling the numerical error of the implicit LOD-FDTD method, where the fast inverse Laplace transform (FILT) is employed to generate the electromagnetic field in arbitrary time domain from that in complex frequency domain. The advantages of our proposed approach are verified in terms of electromagnetic scattering from an array of dispersive gold cylinders [5], [6].

II. FORMULATION

First, we briefly explain the computational process of the conventional LOD-FDTD method to obtain the transient response. Taking into account the dispersion of the Drude model [7], we obtain the equation for the conventional LOD-FDTD method [8] with the aid of the auxiliary differential equation technique [9], [10] as follows:

In the first step ($t = (n + 1/2)\Delta t$),

$$E_x^{n+1/2} = E_x^n, \quad (1)$$

$$E_y^{n+1/2} = E_y^n - \frac{\Delta t}{2\varepsilon_0\varepsilon_\infty} \left(\frac{\partial H_{zx}^{n+1/2}}{\partial x} + \frac{\partial H_{zx}^n}{\partial x} \right) - \frac{\Delta t}{2\varepsilon_0\varepsilon_\infty} \left(J_y^{n+1/2} + J_y^n \right), \quad (2)$$

$$H_{zx}^{n+1/2} = H_{zx}^n - \frac{\Delta t}{2\mu_0} \left(\frac{\partial E_y^{n+1/2}}{\partial x} + \frac{\partial E_y^n}{\partial x} \right), \quad (3)$$

$$H_{zy}^{n+1/2} = H_{zy}^n, \quad (4)$$

$$J_x^{n+1/2} = \frac{2 - \gamma\Delta t}{2 + \gamma\Delta t} J_x^n + \frac{\varepsilon_0\omega_p^2\Delta t}{2 + \gamma\Delta t} \left(E_x^{n+1/2} + E_x^n \right), \quad (5)$$

$$J_y^{n+1/2} = J_y^n. \quad (6)$$

In the second step ($t = (n + 1)\Delta t$),

$$E_x^{n+1} = E_x^{n+1/2} + \frac{\Delta t}{2\varepsilon_0\varepsilon_\infty} \left(\frac{\partial H_{zy}^{n+1}}{\partial y} + \frac{\partial H_{zy}^{n+1/2}}{\partial y} \right) - \frac{\Delta t}{2\varepsilon_0\varepsilon_\infty} \left(J_x^{n+1} + J_x^{n+1/2} \right), \quad (7)$$

$$E_y^{n+1} = E_y^{n+1/2}, \quad (8)$$

$$H_{zx}^{n+1} = H_{zx}^{n+1/2}, \quad (9)$$

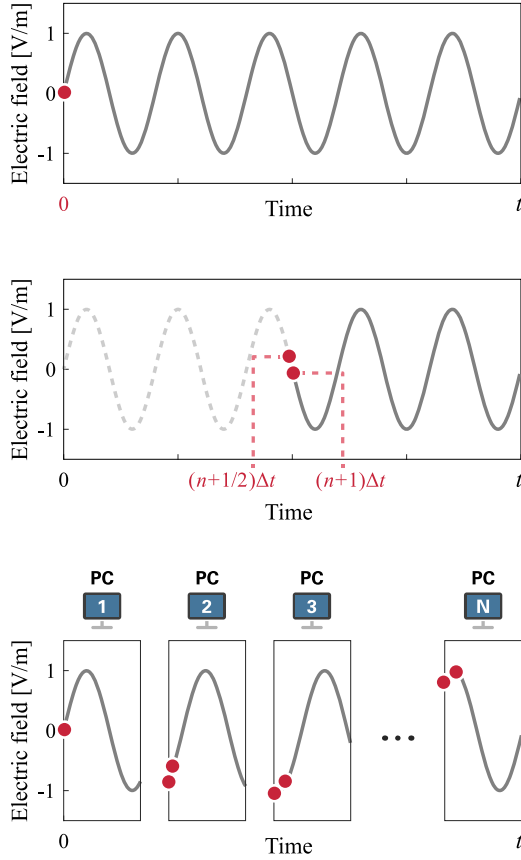


Fig. 1. Examples of the analysis in the conventional and modified LOD-FDTD methods. (a) Conventional LOD-FDTD with an initial value of $t = 0$. (b) Modified LOD-FDTD started at an arbitrary step with initial values of $t = (n + 1/2)\Delta t$ and $t = (n + 1)\Delta t$. (c) Modified LOD-FDTD parallelized with N nodes.

$$H_{zy}^{n+1} = H_{zy}^{n+1/2} + \frac{\Delta t}{2\mu_0} \left(\frac{\partial E_x^{n+1}}{\partial y} + \frac{\partial E_x^{n+1/2}}{\partial y} \right), \quad (10)$$

$$J_x^{n+1} = J_x^{n+1/2}, \quad (11)$$

$$J_y^{n+1} = \frac{2 - \gamma\Delta t}{2 + \gamma\Delta t} J_y^{n+1/2} + \frac{\varepsilon_0 \omega_p^2 \Delta t}{2 + \gamma\Delta t} (E_y^{n+1} + E_y^{n+1/2}), \quad (12)$$

where Δt is the timestep; ε_0 and μ_0 are the permittivity and permeability in free space, respectively; ε_∞ is the relative permittivity at infinite frequency; ω_p is the plasma frequency; and γ is the damping constant. Let us consider a simple example of the electric field evolution over time. In the conventional method shown in Fig. 1(a), given the initial values for the electromagnetic field and current of zero for $t \leq 0$, the subsequent unknowns are updated every half step using the above equations. In this sequential process, a computational error arises owing to the first-order error in time. The main numerical error considered in this study is due to the operator splitting, which was discussed in [12]–[14].

We now introduce an error control approach for the LOD-FDTD method. As shown in Fig. 1(b), the computation can be started at an arbitrary step by providing the initial values of

$n + 1/2$ ($t = (n + 1/2)\Delta t$) and $n + 1$ ($t = (n + 1)\Delta t$) [11]. To obtain the corresponding fields, which will be represented by (20) and (21), we adopt the finite-difference complex-frequency-domain (FDCFD) method [15] with the FILT [16].

In the former FDCFD part, we assume the time dependence of Maxwell's equations to be e^{st} , where $s (= \sigma + j\omega)$ is a complex frequency. Considering the two-dimensional TE case, we obtain the following forms:

$$\frac{\partial E_y}{\partial x} + s\mu_0 H_{zx} = 0, \quad (13)$$

$$-\frac{\partial E_x}{\partial y} + s\mu_0 H_{zy} = 0, \quad (14)$$

$$-\left(\frac{\partial H_{zx}}{\partial x} + \frac{\partial H_{zy}}{\partial x} \right) - s\varepsilon_0 \varepsilon_r(s) E_y = 0, \quad (15)$$

$$\frac{\partial H_{zx}}{\partial y} + \frac{\partial H_{zy}}{\partial y} - s\varepsilon_0 \varepsilon_r(s) E_x = 0. \quad (16)$$

For the dispersive medium described in the Drude model, the relative permittivity in the complex frequency domain (CFD) $\varepsilon_r(s)$ is given as follows:

$$\varepsilon_r(s) = \varepsilon_\infty + \frac{\omega_p^2}{s^2 + s\gamma}. \quad (17)$$

The electric currents in the dispersive media J_x and J_y are calculated using the following equation:

$$\begin{bmatrix} J_x \\ J_y \end{bmatrix} = s\varepsilon_0 (\varepsilon_r(s) - \varepsilon_\infty) \begin{bmatrix} E_x \\ E_y \end{bmatrix}. \quad (18)$$

Furthermore, using the FDCFD method, the steady-state response can be obtained by replacing s with $j\omega$.

After determining the field distribution in the CFD, it is transformed into a time-domain result using the FILT algorithm with double Euler transformation [17]. The following equations give the approximate values $f_{ec}^{n+1/2}$ and f_{ec}^{n+1} in the time domain:

$$f_{ec}^\ell = \frac{e^\alpha}{\ell\Delta t} \left(\begin{array}{l} \sum_{m=k_1}^{k_2} F_m + \frac{1}{A_{p0}} \sum_{m_e=1}^p A_{pm_e} F_{k_2+m_e} \\ + \frac{1}{A_{q0}} \sum_{m_e=1}^q A_{q(m_e)} F_{k_1-m_e} \end{array} \right) \quad (19)$$

where

$$\ell = n + 1/2, n + 1,$$

$$f_{ec}^{n+1/2} = \left[E_y^{n+1/2}, H_{zx}^{n+1/2}, J_x^{n+1/2} \right]^T, \quad (20)$$

$$f_{ec}^{n+1} = \left[E_x^{n+1}, H_{zy}^{n+1}, J_y^{n+1} \right]^T, \quad (21)$$

$$F_m = (-1)^m \text{Im} [F(s)], s = \frac{\alpha + j(m - 0.5)\pi}{\ell\Delta t}, \quad (22)$$

$$\begin{aligned} A_{pp} &= 1, A_{p0} = 2^p, A_{pm_e} \\ &= A_{pm_e-1} - \frac{(p+1)!}{m_e!(p+1-m_e)!}, \end{aligned} \quad (23)$$

α is the approximation parameter; k_1 and k_2 are the lower and upper truncation numbers, respectively; p and q are the number of terms in the Euler transformation; and $F(s)$ represents the

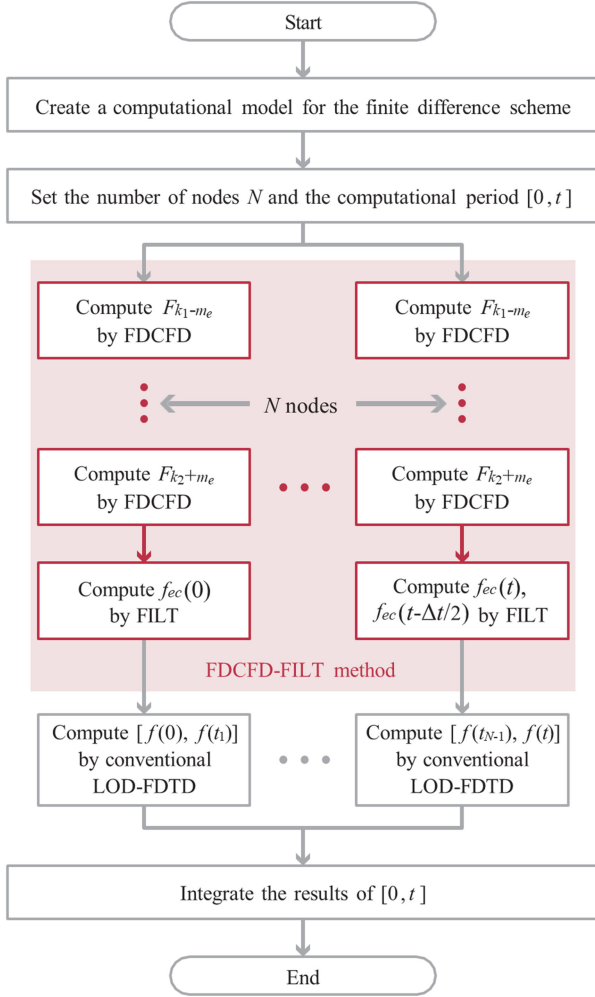


Fig. 2. Flowchart of the modified LOD-FDTD method. The time-division parallel computing is achieved by combining the FDCFD-FILT and LOD-FDTD.

component of the electromagnetic field and electric current in the CFD.

By repeating the above procedures N times, we can perform the time division of the LOD-FDTD method, as shown in Fig. 1(c), which enables parallel computation on N computers. Furthermore, at the beginning of each subsection, the accumulation of a numerical error mainly caused by the operator splitting for the LOD-FDTD method can be controlled and reduced to that from the explicit FDTD method [17]. This leads to a modified LOD-FDTD method, in which the numerical error is reduced with the timestep size.

Fig. 2 shows the flowchart of the proposed method. The time-division parallel computing is achieved by combining the FDCFD-FILT and LOD-FDTD. The corresponding fields for each computational node can be obtained via FDCFD-FILT. They are computed without previous information. Using the obtained initial fields, the numerical error accumulation for LOD-FDTD can be removed.

III. COMPUTATIONAL RESULTS

We analyze the scattering from an array of gold cylinders irradiated with a continuous 500-nm wave, which is the excitation

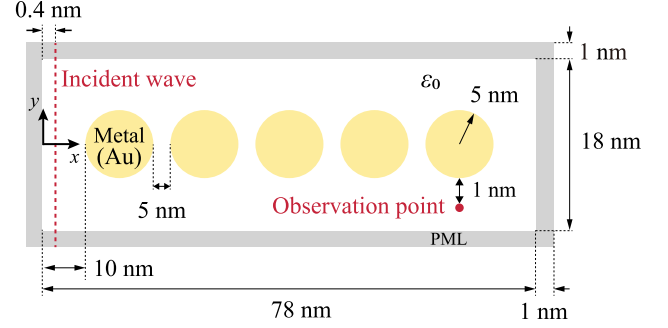


Fig. 3. Computational model with gold cylinders.

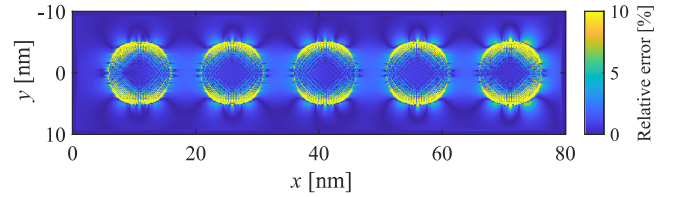


Fig. 4. Relative error in the field component E_y at 40 fs between the conventional LOD-FDTD and CFLN 10 and FDTD.

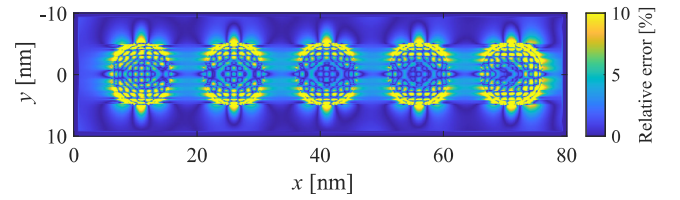


Fig. 5. Relative error in the field component E_y at 40 fs between the conventional LOD-FDTD and CFLN 30 and FDTD.

wavelength of the plasmons. The gold cylinders shown in Fig. 3 form the computational model, which is used as a benchmark. In this model, the cell size is $\Delta x = \Delta y = 0.1$ nm, and the number of cells is $N_x \times N_y = 800 \times 200$, including ten points of perfectly matched layers in both the x - and y -directions. We choose the gold parameters described in the Drude model [18] as follows: $\epsilon_\infty = 9.0685$, $\omega_p = 2155.6$ THz, and $\gamma = 18.36$ THz. In this section, we calculate the time response from $t = 0$ to 50 fs until a steady state is reached.

First, we investigate the accuracy of the conventional LOD-FDTD method compared to the explicit FDTD method. The timestep of the explicit FDTD is set to $\Delta t = 2 \times 10^{-19}$ s to satisfy the CFL condition, and this reference solution is denoted as CFLN 1. The relative errors of the LOD-FDTD method with a timestep of $\Delta t = 2 \times 10^{-18}$ s (CFLN 10) and $\Delta t = 6 \times 10^{-18}$ s (CFLN 30) are compared with the results of the explicit FDTD, as shown in Figs. 4 and 5, respectively. In Fig. 4, we compare the E_y field distributions at $t = 40$ fs; the maximum error is over 10% in the vicinity of the cylinders. It can also be observed that enlarging the CFLN further increases the error, as shown in Fig. 5.

Similarly, the modified LOD-FDTD is applied to the analysis. We refer to the case for the observation time divisions with $N = 100$ nodes parallelized per 0.5 fs. The FILT parameters are the approximation parameter of $\alpha = 5$, truncation number of $k_2 -$

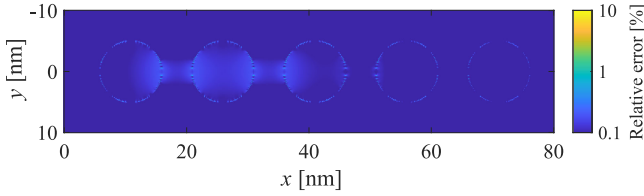


Fig. 6. Relative error in the field component E_y at 40 fs between the modified LOD-FDTD and FDTD.

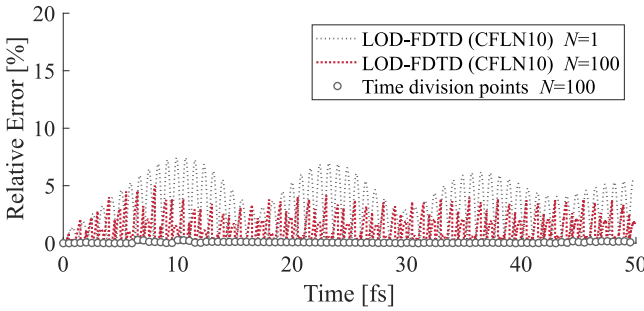


Fig. 7. Time response waveform of E_y obtained from the conventional and modified LOD-FDTD methods for CFLN 10.

$k_1 = 15$, and number of terms in the double Euler transform of $p = q = 5$. Fig. 6 illustrates the relative error of the modified LOD-FDTD compared with the explicit FDTD at $t = 40$ fs. In the entire computational domain, the error is less than 1%.

We then observe the errors arising over time. As shown in Fig. 3, we set an observation point 1 nm from the cylinder, where the magnitude of the electric field is the largest. First, we set the CFLN of the LOD-FDTD to 10. The time response of the electric field E_y is shown in Fig. 7, and the relative error is shown in Fig. 8. When $N = 1$, the error increases with time, and the maximum error is approximately 8%. By contrast, with the modified LOD-FDTD, i.e., when $N = 100$, the error is corrected every 0.5 fs, and the maximum error is reduced to less than 5%. The results for CFLN 30 with $N = 1$ and 200 are shown in Fig. 9. Even with an increasing CFLN, the maximum error is reduced from 15% to 8% by increasing the number of nodes. Note that the observation point is selected at the point where one of the largest errors occurs. Even in this worst case, the relative error can be reduced compared to the conventional LOD-FDTD. As can be seen in Figs. 8(b) and 9(b), there is an error mismatch at the point where the node switches. Since this mismatch is less than the original LOD-FDTD error, its effect on the frequency- and time-domain responses may be negligible. Nevertheless, this effect should be checked, which will be our future work.

We also evaluate the effects of parallel computing in terms of efficiency. The computation times for the proposed method using multiple computers are shown in Fig. 10. As the number of nodes increases, the computation time converges to approximately 250 s, which corresponds to the time required to solve the FDCFD-FILT, causing a bottleneck.

Fortunately, we have realized that the summation in (19) can be performed independently so that the FDCFD-FILT can also be parallelized. In this case, the number of nodes N is split into

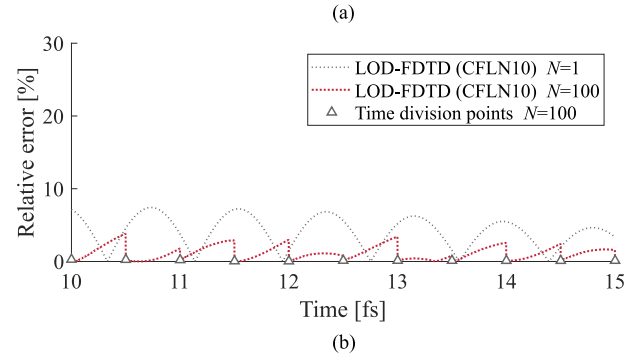
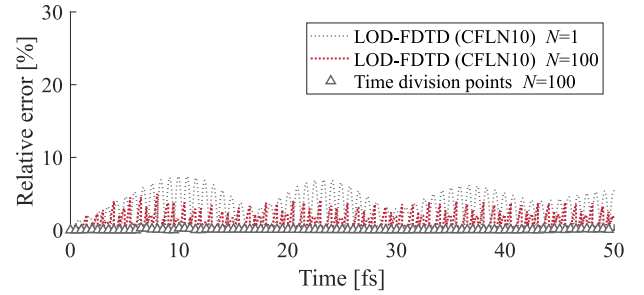


Fig. 8. Relative error of both the conventional and modified LOD-FDTD methods (CFLN 10) compared with that of the FDTD. (a) The observation time is from $t = 0$ to 50 fs. (b) The observation time is from $t = 10$ to 15 fs.

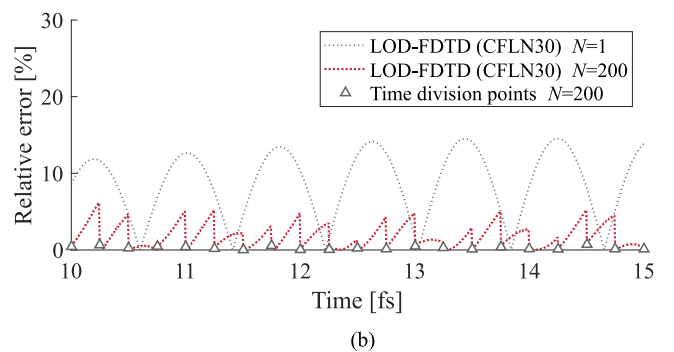
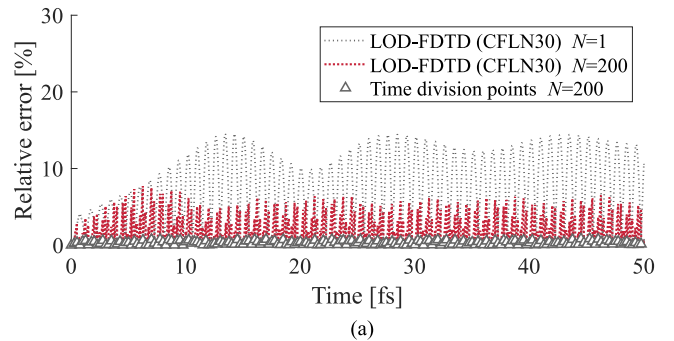


Fig. 9. Relative error of both the conventional and modified LOD-FDTD methods (CFLN 30) compared with that of the FDTD. (a) The observation time is from $t = 0$ to 50 fs. (b) The observation time is from $t = 10$ to 15 fs.

divisions of the LOD-FDTD N_{LOD} and those of the FDCFD-FILT N_{FILT} as follows:

$$N = N_{\text{FILT}} N_{\text{LOD}}. \quad (24)$$

Here, we can optimize N_{FILT} and N_{LOD} such that the computation time T in each node is minimized. This can be estimated

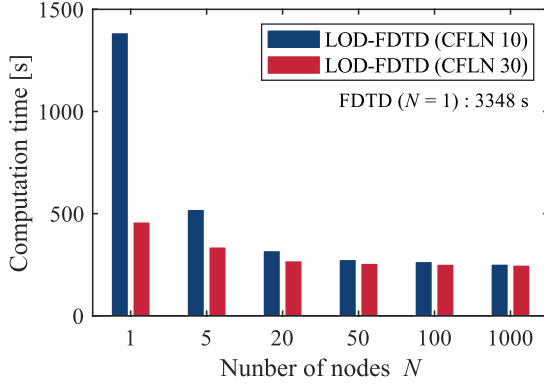


Fig. 10. Calculation time with LOD-FDTD parallelization alone.

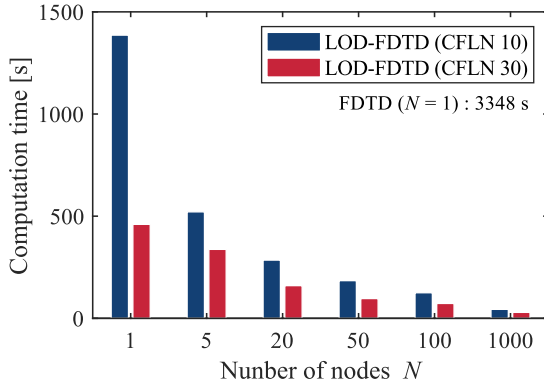


Fig. 11. Calculation time with both the FDCFD-FILT and LOD-FDTD parallelization.

as follows:

$$T = \frac{T_{\text{FILT}}}{N_{\text{FILT}}} + \frac{T_{\text{LOD}}}{N_{\text{LOD}}}, \quad (25)$$

where T_{LOD} and T_{FILT} are the computation times of the LOD-FDTD and FDCFD-FILT without parallelization, respectively. The overall T_{FILT} and T_{LOD} are evaluated by performing several calculation steps, i.e., only a part of the analysis. In the present case, $T_{\text{LOD}} = 1386$ (CFLN 10) and 460 s (CFLN 30), and $T_{\text{FILT}} = 246$ s. From (20) and (21), it is clarified that the value of T is minimum when

$$N_{\text{FILT}} = \text{int} \left(\sqrt{\frac{N T_{\text{FILT}}}{T_{\text{LOD}}}} \right), \quad N_{\text{LOD}} = \text{int} \left(\sqrt{\frac{N T_{\text{LOD}}}{T_{\text{FILT}}}} \right). \quad (26)$$

Note that N_{FILT} and N_{LOD} must be combinations of the divisor of N . The optimized calculation times after the procedure are shown in Fig. 11. In addition, Table I show the N_{FILT} and N_{LOD} calculated using (26). Consequently, the parallelization of both the LOD-FDTD and FDCFD-FILT improves the computational performance, even when the number of nodes increases.

IV. CONCLUSION

We have proposed an error-controllable scheme for the locally one-dimensional finite-difference time-domain method. Implementation of this scheme based on time-division parallel computing can improve its numerical accuracy. The time-division parallel computing can be achieved by using the finite-difference

TABLE I
RESULTS OF NODE OPTIMIZATION FOR N_{FILT} AND N_{LOD}
FOR CFLN 10 AND CFLN 30

CFLN 10						
N	1	5	20	50	100	1000
N_{FILT}	1	1	2	2	4	10
N_{LOD}	1	5	10	25	25	100
CFLN 30						
N	1	5	20	50	100	1000
N_{FILT}	1	1	4	5	5	20
N_{LOD}	1	5	5	10	20	50

complex-frequency-domain with fast inverse Laplace transform. Using the obtained initial fields for each computational node, the numerical error accumulation is satisfactorily removed. In addition, optimal control of the nodes involved in the proposed scheme leads to a significant reduction in computational time, even when multiple nodes are utilized. Certainly, the proposed scheme can be applied to problems with non-dispersive media, as well as problems with and without an electromagnetic source. Moreover, it can also be combined with other implicit solutions, such as the alternating-direction implicit scheme [12]–[14]. Furthermore, it can be extended to three-dimensional problems [19], which we will investigate in future work.

APPENDIX

To obtain the initial fields for each computational node, the fields in the complex-frequency domain are transformed using fast inverse Laplace transform (FILT). In this algorithm, the instantaneous value at a single moment in time is accurately obtained, and the sampling complex frequency can be directly determined. The inverse Laplace transform is defined as the Bromwich integral,

$$f(t) = \frac{1}{2\pi i} \int_{\gamma-i\infty}^{\gamma+i\infty} F(s) e^{st} ds \quad (A1)$$

in which t is the observation time and $F(s)$ is the image function. To perform numerical computation of the Bromwich integral, the cosine in hyperbolic function is applied to exponential function for approximation.

$$e^{st} \approx \frac{e^\alpha}{2 \cosh(st - \alpha)} \quad (A2)$$

Here, α is the approximation parameter. Equation (A2) can be expanded in following series expansion,

$$\frac{e^\alpha}{2 \cosh(st - \alpha)} = \frac{e^\alpha}{2} \sum_{k=-\infty}^{\infty} \frac{(-1)^k}{s - \frac{[\alpha + i(k-0.5)\pi]}{t}} \quad (A3)$$

for $\text{Re}[s] < \alpha$. The singular points of (A3) can be easily given by

$$s_n = \frac{\alpha + i(n-0.5)\pi}{t}, \quad n = 0, \pm 1, \pm 2, \dots \quad (A4)$$

By substituting (A3) and (A4) into the Bromwich integral and using the residue theorem, the approximated time domain function $f_{ap}(t, \alpha)$ is evaluated using the following equation:

$$f_{ap}(t, \alpha) = \frac{e^{\alpha t}}{t} \sum_{n=1}^k F_n, \quad (\text{A5})$$

where

$$F_n = (-1)^n \text{Im} [F(s)], \quad s = \frac{\alpha + i(n - 0.5)\pi}{t},$$

The accuracy of f_{ec} can be controlled by an approximation parameter α . The time-domain function at specific observation time t can be directly computed with (A5). It is worth noting that it is computed without information from the previous time.

REFERENCES

- [1] K. Yee, "Numerical solution of initial boundary value problems involving Maxwell's equations in isotropic media," *IEEE Trans. Antennas Propag.*, vol. AP-14, no. 3, pp. 302–307, May 1966, doi: [10.1109/TAP.1966.1138693](https://doi.org/10.1109/TAP.1966.1138693).
- [2] A. Taflov and S. C. Hagness, "Numerical dispersion and stability," in *Computational Electrodynamics: The Finite-Difference Time-Domain Method*, 3rd ed. Norwood, MA, USA: Artech House, 2005, pp. 107–167.
- [3] J. Shibayama, M. Muraki, J. Yamauchi, and H. Nakano, "Efficient implicit FDTD algorithm based on locally one-dimensional method," *Electron. Lett.*, vol. 41, no. 19, pp. 1046–1047, 2005, doi: [10.1049/el:20052381](https://doi.org/10.1049/el:20052381).
- [4] J. Shibayama, R. Takahashi, J. Yamauchi, and H. Nakano, "Frequency-dependent LOD-FDTD implementations for dispersive media," *Electron. Lett.*, vol. 42, no. 19, pp. 1084–1086, 2006, doi: [10.1049/el:20062383](https://doi.org/10.1049/el:20062383).
- [5] Y. Ando, M. Endo, D. Wu, T. Yamaguchi, S. Kishimoto, and S. Ohnuki, "Design of metallic nanocylinder array waveguide for controlling resonant wavelength shift," *Electron. Lett.*, vol. 57, no. 19, pp. 741–743, 2021, doi: [10.1049/ell2.12241](https://doi.org/10.1049/ell2.12241).
- [6] K. Nagasawa, T. Takeuchi, and S. Ohnuki, "Nonlocal effects occurred in the metallic nano chain driven by longitudinal or transverse modes," *IEICE Electron. Exp.*, vol. 13, no. 8, pp. 1–7, 2016, doi: [10.1587/elex.13.20160216](https://doi.org/10.1587/elex.13.20160216).
- [7] A. D. Rakić, A. B. Djurišić, J. M. Elazar, and M. L. Majewski, "Optical properties of metallic films for vertical-cavity optoelectronic devices," *Appl. Opt.*, vol. 37, no. 22, pp. 5271–5283, 1998, doi: [10.1364/ao.37.005271](https://doi.org/10.1364/ao.37.005271).
- [8] T. Liang, W. Shao, S. Shi, and H. Ou, "Analysis of extraordinary optical transmission with periodic metallic gratings using ADE-LOD-FDTD method," *IEEE Photon. J.*, vol. 8, no. 5, Oct. 2016, Art. no. 7804710, doi: [10.1109/JPHOT.2016.2611698](https://doi.org/10.1109/JPHOT.2016.2611698).
- [9] T. Kashiwa and I. Fukai, "A treatment by the FD-TD method of the dispersive characteristics associated with electronic polarization," *Microw. Opt. Technol. Lett.*, vol. 3, no. 6, pp. 203–205, 1990, doi: [10.1002/mop.4650030606](https://doi.org/10.1002/mop.4650030606).
- [10] T. Yamaguchi and T. Hinata, "Optical near-field analysis of spherical metals: Application of the FDTD method combined with the ADE method," *Opt. Exp.*, vol. 3, no. 6, pp. 11481–11491, 2007, doi: [10.1364/oe.15.011481](https://doi.org/10.1364/oe.15.011481).
- [11] S. Ohnuki, R. Ohnishi, D. Wu, and T. Yamaguchi, "Time-division parallel FDTD algorithm," *IEEE Photon. Technol. Lett.*, vol. 30, no. 24, pp. 2143–2146, Dec. 2018, doi: [10.1109/LPT.2018.2879365](https://doi.org/10.1109/LPT.2018.2879365).
- [12] S. G. Garcia, T.-W. Lee, and S. C. Hagness, "On the accuracy of the ADI-FDTD method," *IEEE Antennas Wireless Propag. Lett.*, vol. 1, pp. 31–34, 2002, doi: [10.1109/LAWP.2002.802583](https://doi.org/10.1109/LAWP.2002.802583).
- [13] M. Darms, R. Schuhmann, H. Spachmann, and T. Weiland, "Dispersion and asymmetry effects of ADI-FDTD," *IEEE Trans. Microw. Wireless Comp. Lett.*, vol. 12, no. 12, pp. 491–493, Dec. 2002, doi: [10.1109/LMWC.2002.805951](https://doi.org/10.1109/LMWC.2002.805951).
- [14] K. Fujita, "Hybrid newmark-conformal FDTD modeling of thin spoof plasmonic metamaterials," *J. Comput. Phys.*, vol. 376, pp. 390–410, 2019, doi: [10.1016/j.jcp.2018.09.050](https://doi.org/10.1016/j.jcp.2018.09.050).
- [15] D. Wu, R. Ohnishi, R. Uemura, and S. Ohnuki, "Finite-difference complex-frequency-domain method for optical and plasmonic analyses," *IEEE Photon. Technol. Lett.*, vol. 30, no. 11, pp. 1024–1027, Jun. 2018, doi: [10.1109/LPT.2018.2828167](https://doi.org/10.1109/LPT.2018.2828167).
- [16] T. Hosono, "Numerical inversion of Laplace transform and some applications to wave optics," *Radio Sci.*, vol. 16, no. 6, pp. 1015–1019, 1981, doi: [10.1029/RS016i006p01015](https://doi.org/10.1029/RS016i006p01015).
- [17] D. Wu, S. Kishimoto, and S. Ohnuki, "Optimal parallel algorithm of fast inverse Laplace transform for electromagnetic analysis," *IEEE Antennas Wireless Propag. Lett.*, vol. 19, no. 12, pp. 2018–2022, Dec. 2020, doi: [10.1109/LAWP.2020.3020327](https://doi.org/10.1109/LAWP.2020.3020327).
- [18] A. Vial, A.-S. Grimault, D. Macías, D. Barchiesi, and M. L. de la Chapelle, "Improved analytical fit of gold dispersion: Application to the modeling of extinction spectra with a finite-difference time-domain method," *Phys. Rev. B*, vol. 71, no. 8, 2005, Art. no. 085416, doi: [10.1103/PhysRevB.71.085416](https://doi.org/10.1103/PhysRevB.71.085416).
- [19] E. L. Tan, "Unconditionally stable LOD-FDTD method for 3-D maxwell's equations," *IEEE Microw. Wireless Compon. Lett.*, vol. 17, no. 2, pp. 85–87, Feb. 2007, doi: [10.1109/LMWC.2006.890166](https://doi.org/10.1109/LMWC.2006.890166).



Tasuku Nakazawa was born in Saitama, Japan, in 1997. He received the B.S. degree in electrical engineering in 2020 from Nihon University, Tokyo, Japan, where he is currently working toward the master's degree. His research focuses on electromagnetic scattering.



Di Wu was born in Xiamen, China, in 1993. He received the B.S., M.S., and Ph.D. degrees in electrical engineering from Nihon University, Tokyo, Japan, in 2016, 2018, and 2021, respectively. His research focuses on computational electromagnetics simulation.



Seiya Kishimoto (Member, IEEE) was born in Chiba, Japan, in 1987. He received the B.S., M.S., and Ph.D. degrees in electrical engineering from Nihon University, Tokyo, Japan, in 2009, 2011, and 2014, respectively. In 2013, he was a Research Fellow of the Japan Society for the Promotion of Science. From 2014 to 2019, he was a Research Scientist with Wireless System Laboratory, Research and Development Center, Toshiba Corporation. In 2019, he joined the Department of Electrical Engineering, College of Science and Technology, Nihon University, where he is currently an Assistant. His research interests include small antennas, tunable antennas, RFID, and fast solvers.



Jun Shibayama (Member, IEEE) was born in Kashiwa, Japan, on July 1, 1969. He received the B.E., M.E., and Dr. E. degrees from Hosei University, Tokyo, Japan, in 1993, 1995, and 2001, respectively. In 1995, he joined Opto-Technology Laboratory, Furukawa Electric Co., Ltd., Ichihara, Japan. In 1999, he became an Assistant of Hosei University, where he is currently a Professor. His research focuses on the numerical analysis of electromagnetic problems. Dr. Shibayama is a Senior Member of the IEICE, and a Member of Optica and ACES.



Junji Yamauchi (Life Fellow, IEEE) was born in Nagoya, Japan, on August 23, 1953. He received the B.E., M.E., and Dr.Eng. degrees from Hosei University, Tokyo, Japan, in 1976, 1978, and 1982, respectively. From 1984 to 1988, he was a Lecturer with the Electrical Engineering Department, Tokyo Metropolitan Technical College, Tokyo, Japan. Since 1988, he has been a member of the Faculty of Hosei University, Tokyo, Japan, where he is currently a Professor. He is the author of *Propagating Beam Analysis of Optical Waveguides* (Research Studies Press, 2003). His research interests include optical waveguides, polarization conversion devices, and circularly polarized antennas.



Shinichiro Ohnuki (Member, IEEE) was born in Tokyo, in 1968. He received the B.S., M.S., and Ph.D. degrees in electrical engineering from Nihon University, Tokyo, Japan, in 1991, 1993, and 2000, respectively. From 2000 to 2004, he was with the Center for Computational Electromagnetics and the Electromagnetics Laboratory, Department of Electrical and Computer Engineering, University of Illinois at Urbana-Champaign, as a Postdoctoral Research Associate and Visiting Lecturer, and later in 2012 as a Visiting Associate Professor. In 2004, he joined the Department of Electrical Engineering, College of Science and Technology, Nihon University, where he is currently a Professor. His research interests include computational electromagnetics and multiphysics simulation.

Dr. Ohnuki was the recipient of the Research Fellowship Award from the Kajima Foundation Tokyo, Japan, in 2000, a corecipient of the Best Paper Award from the Magnetic Society of Japan in 2013, Technical Development Award from the Institute of Electrical Engineers of Japan in 2014, recipient of the Electronics Society Award from the Institute of Electronics, Information and Communication Engineers in 2020. He has been an Editorial Board of Progress in Electromagnetics Research since 2017, an Editorial Advisory Board of Wiley's *International Journal of Numerical Modeling: Electronic Networks, Devices and Fields* since 2020, and was an Associate Editor for the IEEE JOURNAL ON MULTISCALE AND MULTIPHYSICS COMPUTATIONAL TECHNIQUES from 2018 to 2020, and the Secretary of URSI Committee Japan and URSI Commission B from 2017 to 2020.